Contents lists available at SciVerse ScienceDirect

Journal of Magnetism and Magnetic Materials

journal homepage: www.elsevier.com/locate/jmmm
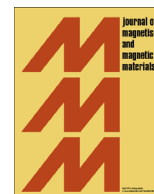
High coercivity induced by mechanical milling in cobalt ferrite powders

Ponce A.S.[a], Chagas E.F.[a,*], Prado R.J.[a], Fernandes C.H.M.[b], Terezo A.J.[b], Baggio-Saitovitch E.[c]

[a] Instituto de Física, Universidade Federal de Mato Grosso, 78060-900, Cuiabá, MT, Brazil
[b] Departamento de Química, Universidade Federal do Mato Grosso, 78060-900, Cuiabá, MT, Brazil
[c] Centro Brasileiro de Pesquisas Físicas, Rua Xavier Sigaud 150 Urca. Rio de Janeiro, Brazil

ARTICLE INFO

ABSTRACT

In this work we report a study of the magnetic behavior of ferrimagnetic oxide $CoFe_2O_4$ treated by mechanical milling with different grinding balls. The cobalt ferrite nanoparticles were prepared using a simple hydrothermal method and annealed at 500 °C. The non-milled sample presented coercivity of about 1.9 kOe, saturation magnetization of 69.5 emu/g, and a remanence ratio of 0.42. After milling, two samples attained coercivity of 4.2 and 4.1 kOe, and saturation magnetization of 67.0 and 71.4 emu/g respectively. The remanence ratio M_R/M_S for these samples increase to 0.49 and 0.51, respectively. To investigate the influence of the microstructure on the magnetic behavior of these samples, we used X-ray powder diffraction (XPD), transmission electron microscopy, and vibrating sample magnetometry. The XPD analysis by the Williamson–Hall plot was used to estimate the average crystallite size and strain induced by mechanical milling in the samples.

1. Introduction

Cobalt ferrite ($CoFe_2O_4$) is a promising compound with potential biomedical applications [1,2], as well as use in high density magnetic storage [3], permanent magnets [4], and electronic devices. This is due to several properties, such as electrical insulation, chemical stability, high magnetic-elastic effect [5], moderate saturation magnetization, and high coercivity (H_C).

Particularly in permanent magnet applications, high H_C is a fundamental characteristic mainly because H_C is an important parameter to the maximum energy product $(BH)_{max}$, the figure of merit for permanent magnets. Many authors report tuning the H_C through thermal annealing [6], capping [7] and mechanical milling treatment [8] of the grains. Limaye et al. [7] obtained cobalt ferrite nanoparticles with very high coercivity (9.5 kOe) by capping it with oleic acid; however, the saturation magnetization decreased to 7.1 emu/g – that is, about 10 times less than that obtained from uncapped nanoparticles. This small value of saturation magnetization (M_S) is an undesirable property in hard magnetic applications. In another interesting article, Liu et al. [9] increased the H_C of cobalt ferrite, from 1.23 to 5.1 kOe, with a relatively small decrease in M_S. They used a brief (1.5 h) mechanical milling process on relatively large particles (average grain size of 240 nm). However, for nanoparticles with an average grain size of 12 nm, no improvement in magnetic parameters was obtained.

Application of mechanical milling to nanoparticles (diameter-< 100 nm) seeking to increase H_C has not yet been successful. However, few important phenomena happen only at the nanoscale. Exchange spring (exchange coupled) is an example. High H_C cobalt ferrite make possible an expressive increase in the $(BH)_{max}$ in exchange coupled nanocomposite $CoFe_2O_4/CoFe_2$ [10,11]. The importance of studying the magnetic behavior of this nanocomposite, aiming to improve its magnetic properties, is what led to this work.

In order to increase the H_C of cobalt ferrite nanoparticles, we processed them with thermal annealing at moderate temperature (500 °C) and brief mechanical milling. Using a shake miller and several different milling parameters, we increased the H_C of all treated samples. The result of this processing was an increase of about 150% in coercivity. Also, the M_R/M_S ratio improved from 0.42 to 0.49 and 0.51 for the two best samples, and the $(BH)_{max}$ was amplified almost 100%. This substantial enhancement in magnetic parameters justifies the publication of this study. Samples were analyzed by X-ray powder diffraction (XPD), transmission electron microscopy (TEM), and magnetic hysteresis curves, all at room temperature.

2. Experimental procedure

The cobalt ferrite nanoparticles were synthesized using a simple hydrothermal method described in a previous work [10]. The morphology and particle size distribution of the samples were examined by direct observation via transmission electron microscopy (TEM) using JEOL-2100 apparatus installed at LNNano/

* Corresponding author. Tel.: +55 65 3615 8747; fax: +55 65 3615 8730.
E-mail addresses: efchagas@fisica.ufmt.br, edschagas@bol.com.br (E.F. Chagas).

Table 1
Details of mechanical milling process.

Sample	Ball material (mass density) (g/cm^3)	Ball diameter (mm)	Proportion ball/sample	Milling time (h)
CF1	Stainless steel 7.8	6.5	1:4	1.5
CF2	Zirconia 6.1	6.0 and 1.2–1.4[a]	1:7:3	1.5
CF3	Zirconia 6.1	6.0	1:7	1.5
CF4	Tungsten carbide 15	5.0	1:9	1.5

[a] The sample CF2 was milled by balls of both indicated sizes.
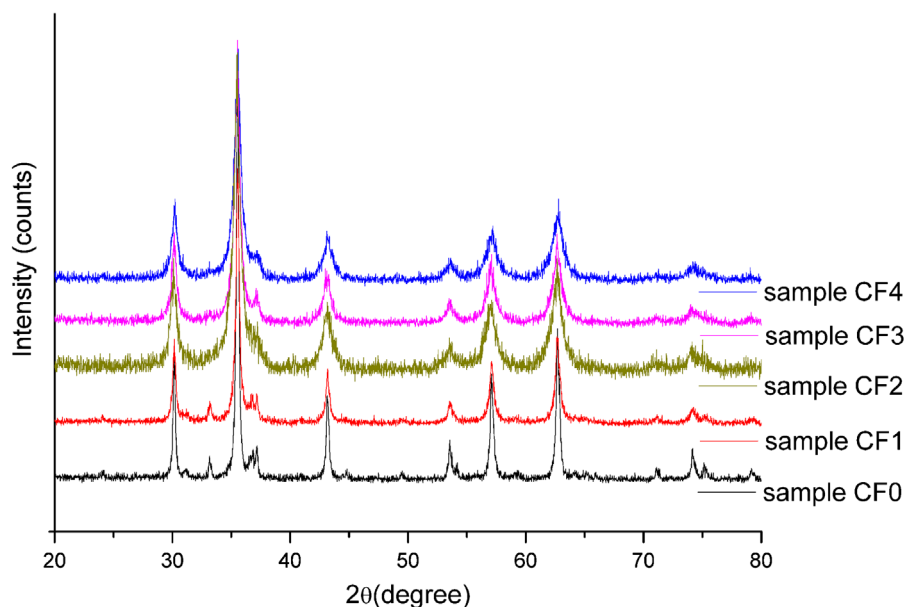
Fig. 1. XPD patterns of Co ferrite.

LNLS–Campinas–Brazil, working at 200 kV, was used for this purpose.

The pristine sample (with neither thermal nor mechanical milling treatments) was annealed at 500 °C for 6 h and separated into 5 amounts called CF0, CF1, CF2, CF3 and CF4. The sample CF0 was not milled while the other samples were milled for 1.5 h using different milling parameters. The milling process used was the high-energy mechanical ball milling in a Spex 8000 miller. Details of the different milling processes for each sample are described in Table 1.

The crystalline phases of the cobalt ferrite nanoparticles were identified by X-ray powder diffraction (XPD) patterns, obtained on a Shimadzu XRD-6000 diffractometer installed at the "*Laboratório Multiusuário de Técnicas Analíticas*" (LAMUTA/ UFMT–Cuiabá-MT–Brazil). It was equipped with graphite monochromator and conventional Cu tube (0.154178 nm), and working at 1.2 kW (40 kV, 30 mA), using the Bragg-Brentano geometry.

Magnetic measurements were carried out using a vibrating sample magnetometer (VSM) model VersaLab Quantum Design, installed at CBPF, Rio de Janeiro-RJ—Brazil. Experiments were done at room temperature and using magnetic field up to 2.5T.

3. Results and discussion

The XPD patterns obtained from samples CF0, CF1, CF2, CF3 and CF4 (see Fig. 1) confirming that all samples are CoFe$_2$O$_4$ with the expected inverse spinel structure. These measurements indicate the absence of any other phases or contamination before and after milling processing.

TEM images of the pristine cobalt ferrite nanoparticles revelead an extremely polydisperse system with several forms (see Fig. 2a). The particle size distribution indicates that cobalt ferrite particles have a mean diameter of 22.6 nm; hovever TEM images also revealed the presence of particles larger than 100 nm. TEM measurements also indicate that nanoparticles increased after thermal treatment, changing the mean diameter to 44.7 nm. As occurred for the pristine sample, some big particles were observed to sample CF0 (Fig. 2b). These results indicate that, despite the relatively low annealing temperature, there was coalescence of nanoparticles causing the increase of mean size.

For samples CF3 and CF4 the TEM images revealed similar particles with shear bands (see the Fig. 3a and b). We observed both regular and irregular shear bands in good agreement with the microstructural evolution described by Liu et al. [9]. These observations suggest that the shear bands are moiré fringes (see Fig. 3c).

To evaluate the influence of mechanical milling on the magnetic behavior of our samples, we measured the magnetic hysteresis loop. These measurements are shown in Fig. 4. Three interesting characteristics can be noted from the hysteresis loops obtained from milled samples: the increase in H_C, the changes in M_S, and the increase of M_R to all milled samples. These characteristics are discussed in detail below.

Samples CF3 and CF4 presented the highest H_C values found in this work, 4.1 and 4.2 kOe, respectively. This enhancement in H_C,
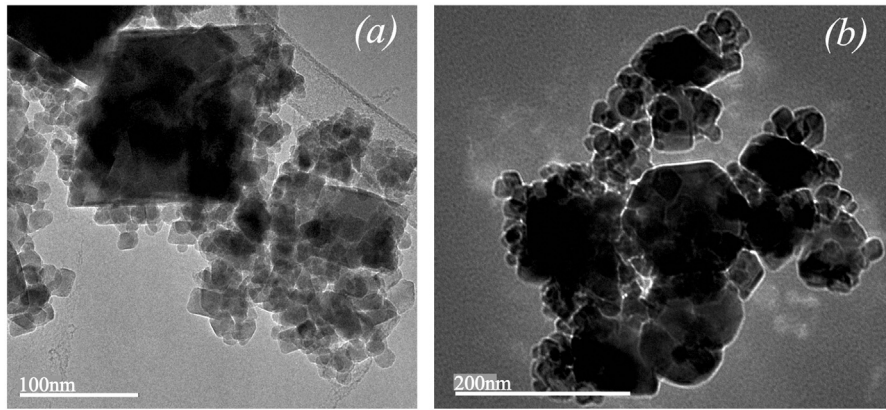
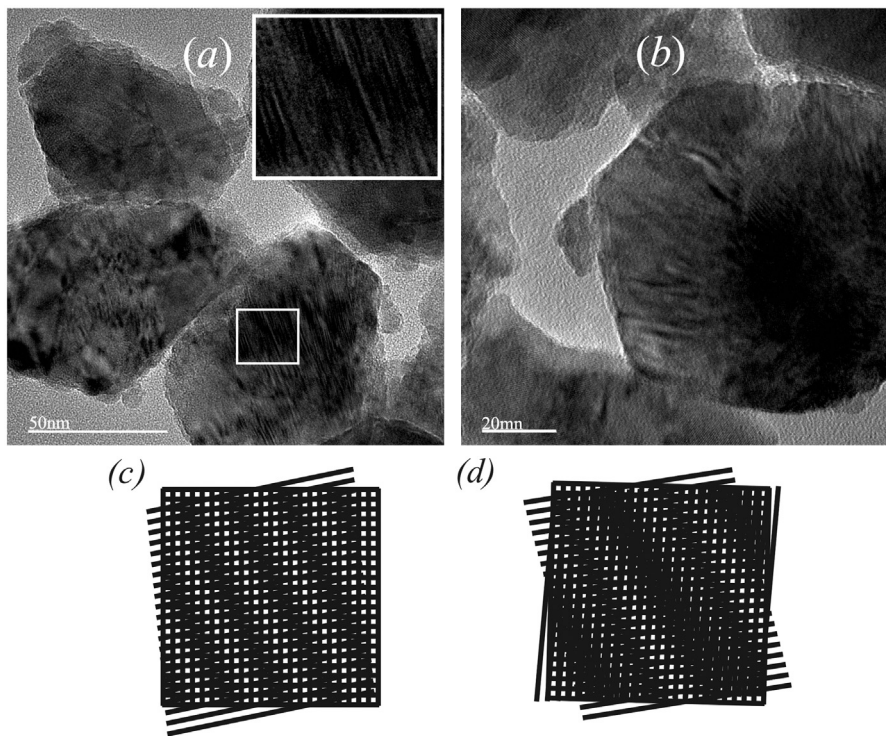**Fig. 2.** TEM images of (a) the pristine sample and (b) sample CF0.

Fig. 3. TEM images showing shear bands observed in (a) CF4 and (b) CF3 samples, and (c) regular and (d) irregular schematic pictures of Moire fringes. The insert in figure (a) shows details of the marked area (showing regular fringes).

when compared with the value obtained for sample CF0 (no mechanical milling), is very expressive and indicates an increase of about 120% after milling, for both samples. However, the maximum energy product for sample CF4 (0.88 MGOe) was smaller than that observed in sample CF3 (1.1 MGOe) due the different M_R for both samples–36.8 emu/g for sample CF3 and 33.0 emu/g for CF4. The main magnetic characteristics obtained for all the samples studied in this work are shown in Table 2.

To investigate the influence of the annealing and milling processes on the strain and average crystallite size of the samples, we used the Williamson–Hall plot [12–14] obtained by the XPD measurements, as in reference [13]. The analysis shows that broadening of the diffraction peaks after milling evidences both grain size reduction and increase in microstructural strain. The instrumental broadening was corrected using the Y_2O_3.diffraction pattern as the standard. The results of the Williamson–Hall plot analysis are shown in Fig. 5.

To facilitate the analysis of the influence of structural parameters on the magnetic behavior of the samples, we included in Table 3 results obtained from the Williamson–Hall analysis together with coercivity and saturation magnetization.

As one can see, milled samples presented a smaller average crystallite size, and microstructural strain-induced by milling was observed in samples CF2, CF3 and CF4. The strain from samples CF0 and CF1 were similar, within the margin of experimental errors of the method. The strain observed in sample CF4 was very close to the value obtained by Liu and Ding [8] for their sample with highest coercivity. The main difference between our sample CF4 and that of Liu and Ding's [8] work is the average size of the particles. In Liu and Ding's work the average particle size was about 110 nm, while in our study it was 21 nm. Besides the mean diameter of the nanoparticles from sample CF4 being smaller than the critical size expected for the magnetic multi-domain regime [15], many big particles with a diameter larger than this critical
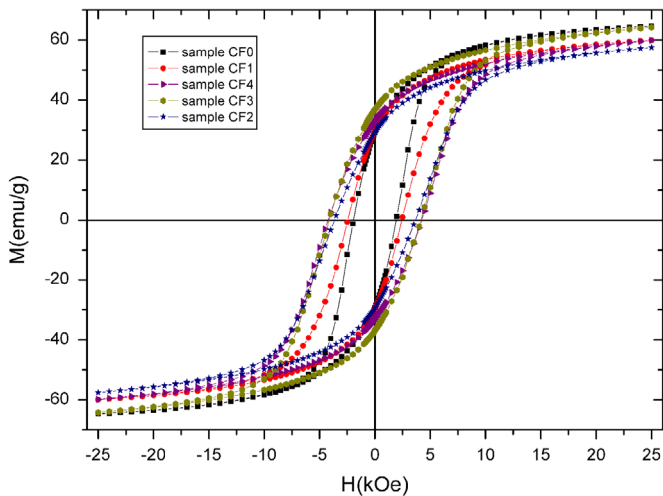
Fig. 4. Hysteresis loops for CoFe$_2$O$_4$ nanoparticles at room temperature (300 K) for maximum applied field of 25 kOe.

Table 2
Magnetic characteristics of milled cobalt ferrite at room temperature.

Sample	Coercivity (kOe)	M_R(emu/g)	M_R/M_S	$(BH)_{max}$ (MG Oe)	M_S(emu/g)
CF0	1.9	29.2	0.42	0.54	69.5
CF1	2.5	29.4	0.44	0.61	66.6
CF2	3.7	29.3	0.45	0.66	64.6
CF3	4.1	36.8	0.51	1.1	71.4
CF4	4.2	33.0	0.49	0.88	67.0
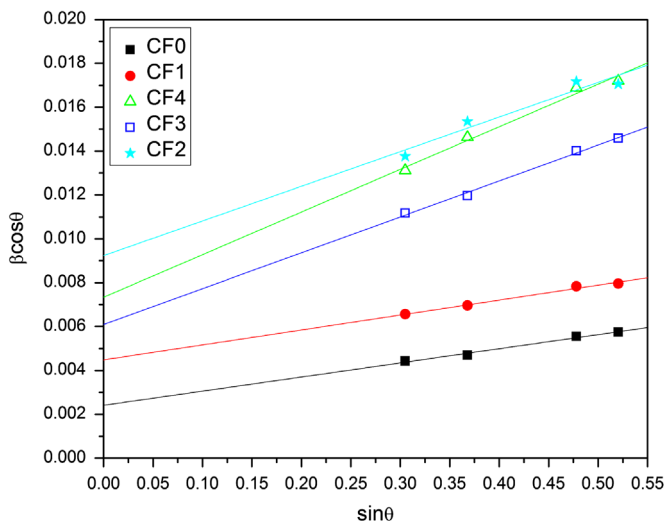
Fig. 5. Willianson–Hall plot to milled cobalt ferrite.

Table 3
Results obtained from Williamson–Hall analysis, coercivity and saturation magnetization.

Sample	Grain size (nm)	Strain (%)	H_C (kOe)	M_S (emu/g)
CF0	64(5)	0.32(3)	1.9	69.5
CF1	34(2)	0.34(3)	2.5	66.6
CF2	17(2)	0.8(1)	3.7	64.6
CF3	25(2)	0.8(1)	4.1	71.4
CF4	21(1)	1.0(1)	4.2	67.0

size were observed in TEM images. Thus we conclude that particles in the multi-domain regime play an important role in magnetic behavior. Pinning effects observed by Liu et al. [9] must also be important to our samples. Structural defects that produce the pinning of wall domains were observed with high magnification TEM measurements (see Fig. 6). We conclude that a combination of strain and pinning effect is responsible for the increase of H_C in sample CF4.

The increase of H_C observed in the other samples (CF1, CF2, and CF3) is clearly associated with the strain induced by mechanical milling. The samples presenting the two highest H_C values, CF3 ($H_C = 4.1$ kOe) and CF4 ($H_C = 4.2$ kOe), also have the largest strains: 0.8 and 1.0, respectively. The sample with lowest H_C, CF1 ($H_C = 2.5$ kOe), presents the smaller strain (0.34). To sample CF3, as to sample CF4, shear bands were observed in TEM images (not showed) suggesting that pinning effect play an important role in the magnitude of H_C also to this sample.

The second important characteristic observed in the hysteresis loops was the change in saturation magnetization (M_S) in the milled samples. The M_S values were obtained by extrapolating $1/H$ to zero in the plot magnetization versus $1/H$. Except for the sample CF3, the M_S decreased in the other milled samples. M_S increased from 69.5 emu/g (sample CF0) to 71.4 emu/g in the sample CF3, but for sample CF2 there was a decrease of about 7.5%. Normally, when M_S decreases together with crystallite size, the decrease in M_S is attributed to the surface effect, sometimes called the "dead" surface [16]. The dead surface is associated with disorder of surface spins. The number of surface spins in a sample increases when the crystallite size decreases, thus it is expected that the M_S will also decrease. However, this explanation is not consistent with all our results. If compared with the non-milled sample CF0, the saturation magnetization of the samples CF1, CF2 and CF4 decreases with the crystallite size, but the M_S for sample CF3 was higher than that obtained for sample CF0 (see Table 3). Thus we attributed the change in saturation magnetization to a combination of two factors: the surface effect [17] and redistribution of magnetic cations [18].

To understand the cation redistribution it is necessary to know the cobalt ferrite structure and the distribution of magnetic ions in this structure. The cobalt ferrite has an inverse spinel structure with the two magnetic ions (Co^{2+} and Fe^{3+}) occupying two different sites called A and B. The A site is a tetrahedral site and the B site is an octahedral site. In an ideal inverse spinel cobalt ferrite, half of the Fe^{3+} cations (magnetic moment equal to 5μ_B) occupy the A-sites and the other half the B-sites, together with Co^{2+} cations. (There are two B sites for formula unit). Since the magnetic moments of the ions in the A and B sites are aligned in
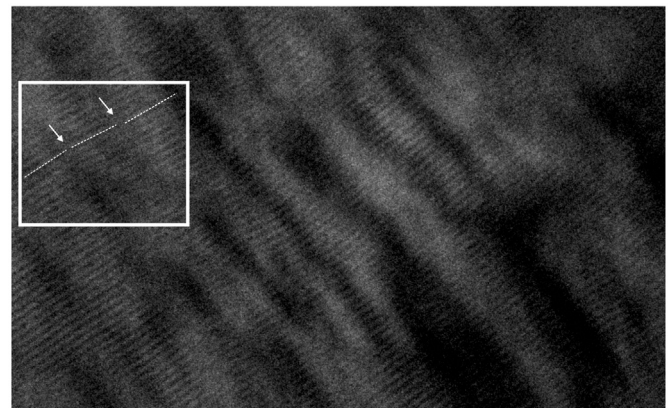
Fig. 6. Structural defects in crystalline plans to milled cobalt ferrite (sample CF4). The marked area indicates a structural defect.

an anti-parallel way, the magnetic contribution of the Fe^{3+} cations are mutually compensated. Therefore, the net magnetic moment of the ideal inverse spinel cobalt ferrite is due only to the Co^{2+} cations (magnetic moment equal to $3\mu B$). However, the cobalt ferrite normally presents a mixed spinel structure, the sites A and B have a fraction of Co^{2+} and Fe^{3+} cations. Therefore, in a general way, the structure of cobalt ferrite can be described by reference [18]:

$$Co_{1-i}^{2+}Fe_i^{3+}[Co_i^{2+}Fe_{2-i}^{3+}]O_4^{2-} \qquad (1)$$

where i (the degree of inversion) describes the fraction of the tetrahedral sites occupied by Fe^{3+} cations. The ideal inverse spinel structure has $i=1$, $i=0$ to the normal spinel and to the mixed spinel structure the value of i is between 0 and 1.

If Co^{2+} ions move from A-sites to B-sites and consequently Fe^{3+} cations move from B-sites to A-sites, there will be a change in the degree of inversion i (see Eq. 1), a decrease of the net magnetic moment of the material, and, consequently, a decrease in M_S. On the other hand, if the opposite process happens the saturation magnetization will increase. In a recent article, Sato Turtelli et al. [18] showed that samples prepared by mechanical milling present an i factor smaller than that obtained for samples synthesized by sol gel method. Another indication that there is a cationic redistribution in $CoFe_2O_4$, due mechanical milling is the work of Stewart et al. [19]. They observed cation swap between magnetic site A and B in normal spinel ferrite $ZnFe_2O_4$ due the mechanical milling. In addition, the cationic redistribution described before is consistent with the enhancement of the H_C due to changes in the magneto-crystalline anisotropy. According to Sato Turtelli et al. [18] more Co^{2+} in B-site (smaller value of i factor) increases the magneto-crystalline anisotropy and, consequently, increases the coercivity.

The third interesting result observed in magnetic measurements is the increase of remanence (M_R) and, consequently, the increase of the remanence ratio (M_R/M_S) obtained for all of the milled samples (see table 2). Sample CF3 presented the most expressive increase of M_R and, consequently, highest M_R/M_S ratio (0.51).

This effect (desirable for hard magnetic applications) is probably due to one of the causes of the increase of coercivity, namely the change in the magnetic anisotropy (primarily the stress anisotropy). For the CF3 sample, changes in the magneto-crystalline anisotropy caused by cationic redistribution, as discussed above, can also contributed to this effect.

There are two other possible causes for the increase of remanence observed for the milled samples. One is that changes of magnetic domain regime of the samples after milling due to a reduction in the average crystallite size, the CF0 sample has an average size of about 65 nm, indicating that this sample is in the magnetic multi-domain regime [15]. Thus the magnetization process is caused mainly by the movement of domain walls. However, when the grain is smaller than 40 nm, as for the milled samples, the cobalt ferrite is in the single magnetic domain regime and the magnetization curve is governed by rotation of the magnetic moments. The moving of domain walls is easier than rotating the magnetic moment of the particles [20,21]. Another possible explanation for the increase of remanence is the enhancement of the cubic magneto-crystalline anisotropy, indicated by the approximation of the expected theoretical value to non-interacting particles with positive cubic anisotropy (0.83 at 0 K) [22], a similar effect occurs when the temperature decreases [10,23], but still not clear, thus this assumption deserves more investigation.

4. Conclusion

In agreement with other authors, our results suggest that strain plays an important role in the H_C value. Structural defects were

observed in big particles (around of 100 nm), these pinning centers must be important to high H_C behavior.

The increase of M_S and M_R observed in sample CF3 compared with not milled sample suggest that high energy ball milling can promote a cationic swap between Co^{2+} and Fe^{3+} from A and B sites respectively. However, this assumption deserves more investigation.

We achieved a significant increase of the $(BH)_{max}$ for sample CF3 compared with non-milled samples due the H_C and the M_R enhancement. The increase of the $(BH)_{max}$ in sample CF4 was smaller, indicating that grinding ball mass density plays an important role in the magnetic behavior of milled samples.

References

[1] M. Colombo, S. Carregal-Romero, M.F. Casula, L. Gutiérrez, M.P. Morales, I. B. Bohm, J.T. Heverhagen, D. Prosperi, W.J. Parak, Biological applications of magnetic nanoparticles, Chemical Society Reviews 41 (2012) 4306–4334.
[2] T.E. Torres, A.G. Roca, M.P. Morales, A. Ibarra, C. Marquina, M.R. Ibarra, G.F. Goya, Magnetic properties and energy absorption of $CoFe_2O_4$ nanoparticles for magnetic hyperthermia, Journal of Physics: Conference Series, 200 (2010) 072101.
[3] V. Pillai, D.O. Shah, Synthesis of high-coercivity cobalt ferrite particles using water-in-oil microemulsions, Journal of Magnetism and Magnetic Materials 163 (1996) 243–248.
[4] Y.C. Wang, J. Ding, J.B. Yi, B.H. Liu, T. Yu, Z.X. Shen, High-coercivity Co-ferrite thin films on (100)-SiO_2 substrate, Applied Physics Letters 84 (2004) 2596–2598.
[5] I.C. Nlebedim, J.E. Snyder, A.J. Moses, D.C. Jiles, Dependence of the magnetic and magnetoelastic properties of cobalt ferrite on processing parameters, Journal of Magnetism and Magnetic Materials 322 (2010) 3938–3942.
[6] W.S. Chiua, S. Radiman, R. Abd-Shukor, M.H. Abdullah, P.S. Khiew, Tunable coercivity of $CoFe_2O_4$ nanoparticles via thermal annealing treatment, Journal of Alloys and Compounds 459 (2008) 291–297.
[7] M.V. Limaye, S.B. Singh, S.K. Date, D. Kothari, V.R. Reddy, A. Gupta, V. Sathe, R. J. Choudhary, S.K. Kulkarni, High coercivity of oleic acid capped $CoFe_2O_4$ nanoparticles at room temperature, Journal of Physical Chemistry B 113 (2009) 9070–9076.
[8] B.H. Liu, J. Ding, Strain-induced high coercivity in $CoFe_2O_4$ powders, Journal of Physical Chemistry B 88 (2006) 042506.
[9] B.H. Liu, J. Ding, Z.L. Dong, C.B. Boothroyd, J.H. Yin, J.B. Yi, Microstructural evolution and its influence on the magnetic properties of $CoFe_2O_4$ powders during mechanical milling, Physical Review B 74 (2006) 184427.
[10] G.C.P. Leite, E.F. Chagas, R. Pereira, R.J. Prado, A.J. Terezo, M. Alzamora, E. Baggio-Saitovich, Exchange coupling behavior in bimagnetic $CoFe_2O_4$/$CoFe_2$ nanocomposite, Journal of Magnetism and Magnetic Materials 324 (2012) 2711–2716.
[11] J.M. Soares, F.A.O. Cabral, J.H. de Araújo, F.L.A. Machado, Exchange-spring behavior in nanopowders of $CoFe_2O_4$–$CoFe_2$, Applied Physics Letters 98 (2011) 072502.
[12] G.K Williamson, W.H. Hall, X ray line broadening from filed aluminium and wolfram 1 (1953) 22–31Acta Metallurgica 1 (1953) 22–31.
[13] V.D. Mote, Y. Purushotham, B.N. Dole, Williamson–Hall analysis in estimation of lattice strain in nanometer-sized ZnO particles, Journal of Theoretical and Applied Physics 6 (2012) 6.
[14] A. Khorsand Zak, W.H.Abd. Majid, M.E. Abrishami, Ramin Yousefi, X-ray analysis of ZnO nanoparticles by Williamson–Hall and size-strain plot methods 13 (2011) 251–256Solid State Science 13 (2011) 251–256.
[15] Debabrata Pal, Madhuri Mandal, Arka Chaudhuri, Bipul Das, Debasish Sarkar, Kalyan Mandal, Micelles induced high coercivity in single domain cobalt-ferrite nanoparticles, Journal of Applied Physics 108 (2010) 124317.
[16] A. Franco, F.C.e Silva, Vivien S. Zapf, High temperature magnetic properties of $Co_{1-x}Mg_xFe_2O_4$ nanoparticles prepared by forced hydrolysis method, Journal of Applied Physics 111 (2012) 07B530.
[17] M. Rajendran, R.C. Pullar, A.K. Bhattacharya, D. Das, S.N. Chintalapudi, C. K. Majumdar, Magnetic properties of nanocrystalline $CoFe_2O_4$ powders prepared at room temperature: variation with crystallite size, Journal of Magnetism and Magnetic Materials 232 (2001) 71–83.
[18] R. Sato Turtelli, M. Atif, N. Mehmooda, F. Kubel, K. Biernacka, W. Linert, R. Grössingera, Cz. Kapusta, M. Sikora, Interplay between the cation

distribution and production methods in cobalt ferrite, Materials Chemistry and Physics 132 (2012) 832–838.

[19] S.J. Stewart, S.J.A. Figueroa, J.M. Ramallo López, S.G. Marchetti, J.F. Bengoa, R.J. Prado, F.G. Requejo, Cationic exchange in nanosized $ZnFe_2O_4$ spinel revealed by experimental and simulated near-edge absorption structure, Physical Review B 75 (2007) 073408.

[20] E.F. Kneller, F.E. Luborsky, Particle size dependence of coercivity and remanence of single domain particles, Journal of Applied Physics 34 (1963) 656–658.

[21] A.P. Guimarães, NanoScience and Technology: Principles of Nanomagnetism, Springer-Verlag, Berlin Heidelberg61.

[22] M.P. Pileni, Size and morphology control of nanoparticles growth in organized surfactant assemblies, in: Janos H. Fendler, Imre Dékány (Eds.), Nanoparticles and Nanostructured Films, Kluwer Academic Publishers, Dordrecht, 1996, p. 80.

[23] E. Veena Gopalan, I.A. Al-Omari, D.Sakthi Kumar, Yasuhiko Yoshida, P.A. Joy, M.R. Anantharaman, Inverse magnetocaloric effect in sol–gel derived nanosized cobalt ferrite, Applied Physics A 99 (2010) 497–503.